91602
new 82-10

COMPLIMENTARY COPY
Please Credit Ontario Hydro Research if Reproduced in Whole or in Part

LEGAL NOTICE

This report was prepared by Ontario Hydro and, while effort has been made to assure the accuracy and applicability of the material contained herein, neither Ontario Hydro nor any person acting on its behalf:

(a) makes any warranty, express or implied with respect to the use of any information, apparatus, method or process disclosed in this report or that such use may not infringe privately owned rights; or

(b) assumes any liabilities with respect to the use of, or for damages resulting from the use of, any information, apparatus, method or process disclosed in this report.

ontario hydro
research division

DARLINGTON GENERATOR ROTOR: FINITE ELEMENT K-CALIBRATION OF A FATIGUE CRACK GROWTH SPECIMEN

Report No. 91-41-K

M.L. Vanderglas - Engineer
Fracture Technology Section
Metallurgical Research Department

ABSTRACT

A three-dimensional elastic finite element analysis of a fatigue crack growth specimen is described. This work was undertaken in support of a material test program to obtain near-threshold fatigue-crack growth rate properties of Darlington generator rotor material. The object of the analysis was to obtain the stress-intensity factor K as a function of crack length and load with particular attention to the effects of the bending restraint imparted by the test fixture. The effect of restraint is to reduce K, an effect which would render measured growth rate versus ΔK curves non-conservative if not taken into account. Appendix A gives a collateral 2D study of the influence of plate length on K for edge-cracked plates with various force, moment, deflection and rotational boundary conditions.

job	file	date	report no.
85-118	826.233	April 12, 1991	91-41-K

91602
new 82-10

ontario hydro
research division

EXECUTIVE SUMMARY

DARLINGTON GENERATOR ROTOR: FINITE ELEMENT K-CALIBRATION OF A FATIGUE CRACK GROWTH SPECIMEN

M.L. Vanderglas
Fracture Technology Section
Metallurgical Research Department

The failure in early 1990 of the Darlington Unit 2 generator rotor shaft prompted, among other things, a material test program to examine the conditions required to initiate a crack in the rotor material. This information will be used to determine the maximum non-initiating crack size in the rotor and thus to set inspection requirements.

The dominant cyclic stresses in the rotor result from reversed bending, arising because the rotor sags between its bearings. Consequently, a specimen was designed to measure crack growth rates due to tension-compression loading. These can be correlated with ΔK the amplitude of stress-intensity factor, K. Specimen testing will determine the initiation threshold value of ΔK at which the growth rate is effectively zero (say 10^{-10} m/cycle or less).

K is a function of load and crack length. This function, the so-called "K-calibration", was not known for the present specimen/load-fixture configuration. This report describes the method by which the K-calibration was determined analytically by finite element analysis and examines in detail the interaction of specimen and load fixture.

B.M
B.M

job	file	date	report no
85-118	826.233	April 12, 1991	91-41-K

TABLE OF CONTENTS

		PAGE
1.0	INTRODUCTION	1
2.0	PRELIMINARY 2D STUDY	1
3.0	METHOD FOR 3D ANALYSIS	2
4.0	3D CASE DESCRIPTIONS	3
5.0	VERIFICATION	5
5.1	Comparison With Test Results	5
5.2	Comparison With Published Results	6
5.3	Internal Consistency Of Results	6
6.0	RESULTS	7
7.0	DISCUSSION	8
8.0	CONCLUSION	8
REFERENCES		9
APPENDIX A	2D FINITE ELEMENT STUDY OF ROTATIONAL CONSTRAINT	10
APPENDIX B	FINITE ELEMENT DETAILS	18
APPENDIX C	CALCULATION OF K BY ALTERNATIVE METHODS	19
C-1	Virtual Crack Extension (VCE)	19
C-2	Displacement Substitution	23
C-3	Compliance	23
APPENDIX D	3D SPECIMEN ANALYSIS - SUMMARY OF RESULTS	27
DISTRIBUTION		last page

LIST OF FIGURES

Figure 1	Specimen Dimensions as Modelled
Figure 2	3D Finite Element Models of Test Specimen
Figure 3	Comparison of Finite Element and Measured Crack-Mouth Opening Deflections (CMOD)
Figure 4	Comparison of Finite Element and Measured Strains
Figure 5	Comparison of Geometry "Corrections" for 2D SEN with 3D Finite Element Results with Various Boundary Conditions
Figure 6	Comparison of Finite Element and Fitted Normalized K
Figure A-1	2D SEN Plate Test Case - Nomenclature
Figure A-2	Comparison of Geometry Correction Factors for 2D SEN Plates With Tension, Bending and Deflection Boundary Conditions - Effect of Plate Length
Figure A-3	2D SEN Plate Test Case - "Deformed" Meshes of Short and Long Plates with Various Boundary Conditions
Figure A-4	Deflections and Rotations in 2D SEN Plates in Tension and Bending - Effect of Plate Length
Figure A-5	Geometry Correction Factors for 2D SEN in Tension with Constrained End Rotation
Figure A-6	Induced Bending Stress in 2D SEN Plates in Tension with Constrained End Rotations
Figure C-1	J-Variations Along Crack Front - Comparison with Plane-Stress and Plane-Strain Results for Edge-Cracked Plate in Tension
Figure C-2	Comparison of VCE and Displacement Substitution Methods - Deflection BC (1.0 mm) Applied at x = 105.6 mm - Case 2U6
Figure C-3	Comparison of K's From VCE and Computed Compliance - Deflection BC (1.0 mm) Applied at x = 105.6 mm - Case 2U6
Figure C-4	Crack Mouth Opening Deflections - Comparison of Finite Element with Plane-Stress and Plane-Strain Solutions

LIST OF TABLES

Table 1 3D Finite Element Model Case Descriptions

Table A-1 Single-Edge Cracked Plate (a/W = 0.5) Showing Effect of Boundary Condition Type and Plate Length on the Stress Intensity Factor and Vertical Deflections

Table D-1 Summary of 3D Finite Element Results

NOMENCLATURE

Variables used throughout this report are listed below. Additional variables will be described as they appear in the text.

a	=	crack length
CMOD	=	crack-mouth opening deflection
E	=	Young's modulus
E'	=	effective modulus = E (plane stress) = $E/(1-\nu^2)$ (plane strain)
f	=	geometry correction factor
h	=	plate height
J	=	J-integral
K	=	stress intensity factor
ΔK	=	cyclic amplitude of stress-intensity factor
P	=	load
t	=	plate or specimen thickness
v	=	vertical deflection
v'	=	rotation
W	=	plate or specimen width
α	=	a/W
ϵ	=	strain
ν	=	Poisson's ratio
σ	=	stress

ontario hydro
research division

TO: Mr. M.A. Machacek
Manager
Darlington Engineering Department

DARLINGTON GENERATOR ROTOR: FINITE ELEMENT K-CALIBRATION OF A FATIGUE CRACK GROWTH SPECIMEN

1.0 *INTRODUCTION*

This report gives an elastic K-calibration of a fatigue crack growth rate specimen used to obtain threshold ΔK values for Darlington NGS generator rotor material. The finite element (FE) method was used to perform the calibration.

Crack growth rates can be correlated with ΔK, the amplitude of K. The purpose of the calibration is to provide a function which relates K to the measured load and crack length.

2.0 *PRELIMINARY 2D STUDY*

Appendix A describes a two-dimensional (2D) FE study of a single-edge notched (SEN) strip with various force and deflection boundary conditions. Results indicated that the K-versus-a calibration for the specimen might be affected by the rotational constraint imparted by the load fixture. If the plate is loaded in tension:

i) a bending stress which tends to close the crack is induced if rotation is partly or completely constrained

ii) the stress-intensity factor for the constrained case is less than that of a plate with no constraint (i.e. such as a pin-loaded SEN)

iii) the difference in bending stress and K between the constrained and unconstrained cases increases with crack length and decreases with plate length.

For "conservatism" the K-calibration should be under-predicted (otherwise the inferred value of ΔK for a test would be too high). In addition, if the difference between an assumed and correct calibration changes with crack length, a plot of crack growth rate versus the assumed ΔK will exhibit an apparent crack-length dependence. Therefore, the reduction of K due to rotational constraint must be considered.

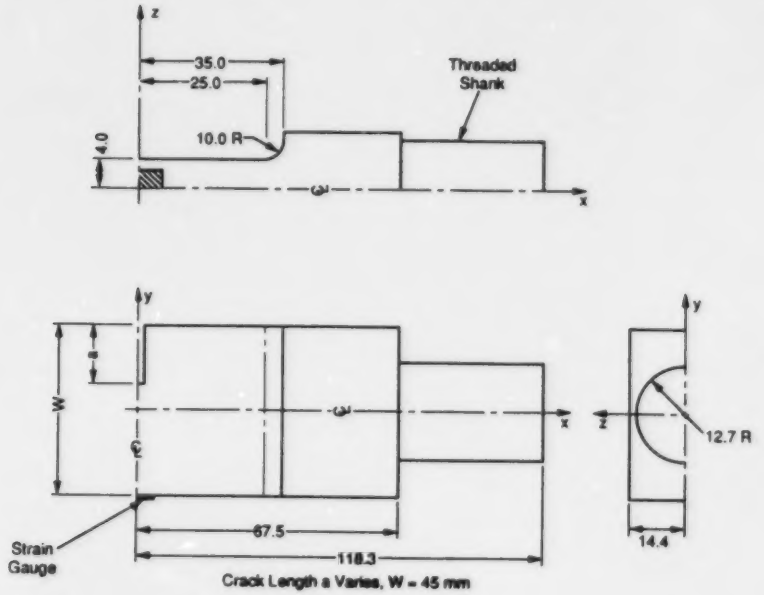

FIGURE 1

SPECIMEN DIMENSIONS AS MODELLED
(DIMENSIONS IN [mm], ROUNDED TO ONE DECIMAL)

3.0 *METHOD FOR 3D ANALYSIS*

The amount of rotational constraint in the specimen/load-fixture arrangement is difficult to quantify. Boundary conditions were varied by trial-and-error until both the computed crack mouth opening deflection (CMOD) and axial back-face strain matched measured values over the required range of crack lengths (a/W = 0.25 to 0.625). Strains were measured at the location shown in Figure 1.

In most cases, the end of the FE model representing the threaded portion was used as a flexural spring. A uniform axial deflection was applied on cross sections at various axial positions. At those sections, no rotation was permitted. Varying the axial position changes the flexural stiffness, thus the rotational constraint applied to the body of the specimen.
The approach is not to "pro-rate" FE results to achieve a match, but to find an "effective" boundary condition which simulates conditions near the crack.

4.0 *3D CASE DESCRIPTIONS*

Specimen dimensions (as modelled) and typical FE models are shown in Figures 1 and 2. Modelling details are given in Appendix B. The 3D cases analyzed are summarized in Table 1. Columns give the following information:

i) column 1 ("case") gives identification codes of form "nxm" in which "n" identifies the model refinement ("1" for coarse, "2" for refined meshes), "x" represents the boundary condition type ("T" for traction, "U" for prescribed deflection) and "m" distinguishes variants with the same type of boundary condition

ii) column 2 gives the values of relative crack lengths analyzed for a given case and model

iii) column 3: most cases were analyzed twice using different values of Poisson's ratio

iv) column 4: description of boundary conditions

TABLE 1
3D Finite Element Model Case Descriptions

case	range of a/W	Poisson's ratio	boundary condition
1T	0.1250 0.2500 0.3750 0.5000 0.6250 0.7500 0.8750	0.0, 0.3	1 MPa traction at end
1U1	0.1250 0.2500 0.3750 0.5000 0.6250 0.7500 0.8750	0.0, 0.3	0.01 mm deflection at end (x = 118.29 mm)
1U2	0.1250 0.2500 0.3750 0.5000 0.6250 0.7500 0.8750	0.0, 0.3	0.01 mm deflection at end, bolt centreline constrained
1U3	0.3750	0.0, 0.3	1 MPa traction at end no shoulder rotation
1U4	0.6250	0.0, 0.3	0.01 mm deflection at x = 73.84 mm
1U5	0.6250 0.7500	0.0, 0.3	0.01 mm deflection at x = 92.88 mm
1U6	0.2500 0.3750 0.5000 0.6250 0.7500	0.0, 0.3	0.01 mm deflection at x = 105.6 mm
2U6	0.2500 0.3125 0.3750 0.4375 0.5000 0.5625 0.6250	0.3	0.01 mm deflection at x = 105.6 mm

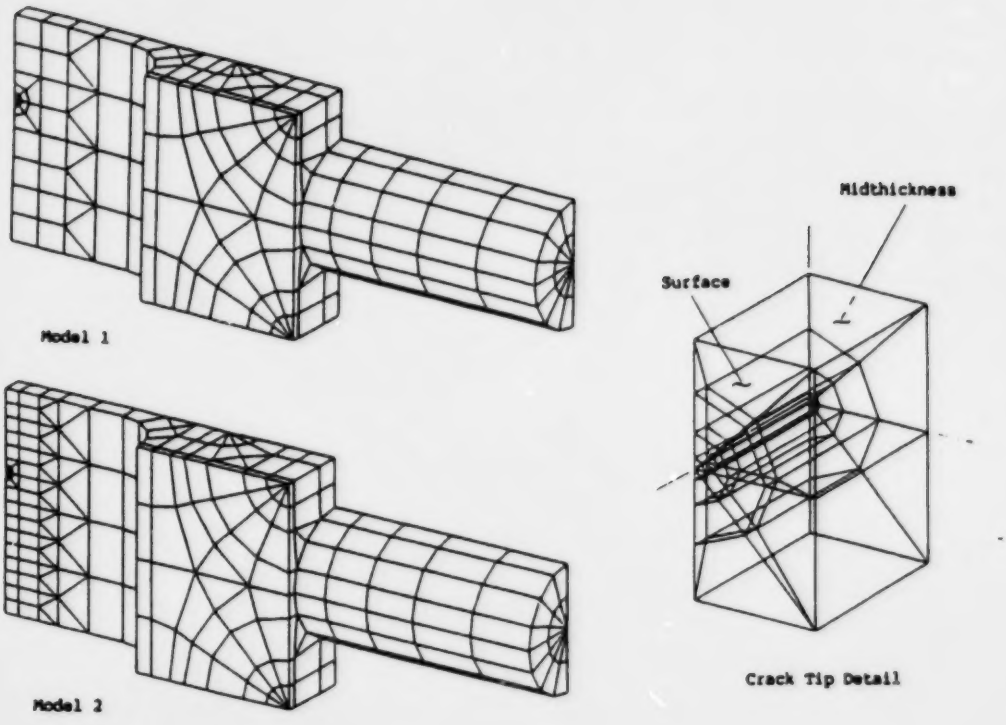

FIGURE 2

3D FINITE ELEMENT MODELS OF TEST SPECIMEN
(MODELS FOR a/W=0.375 SHOWN)

Cases with tensile loading ("1T") had no rotational constraint. These were used for model verification, to be compared to similar 2D SEN plate solutions.

Cases "1U1" through "1U3" were analyzed to gain some appreciation of model response to different types of rotational constraint.

Cases "1U4" through "1U6" were studied to iteratively refine the axial location at which to apply the deflection boundary condition to match test results.

Case "2U6", a refined-mesh version of "1U6", was used to check the convergence of FE results.

5.0 *VERIFICATION*

The FE model should agree with test results, available published analytical results, and be internally consistent.

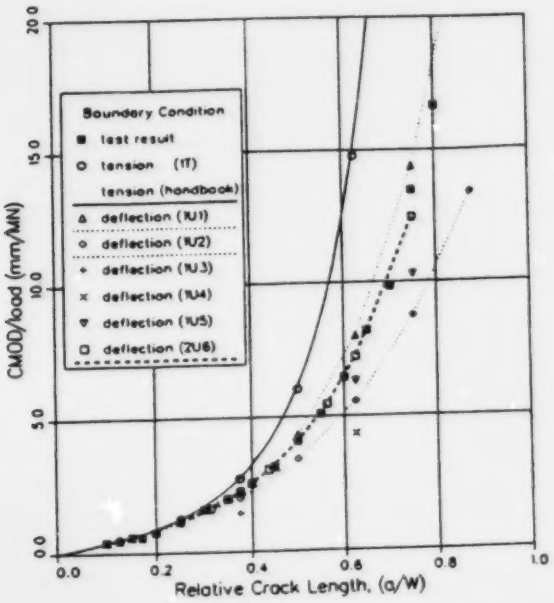

FIGURE 3

COMPARISON OF FINITE ELEMENT AND MEASURED CRACK-MOUTH OPENING DEFLECTIONS (CMOD)

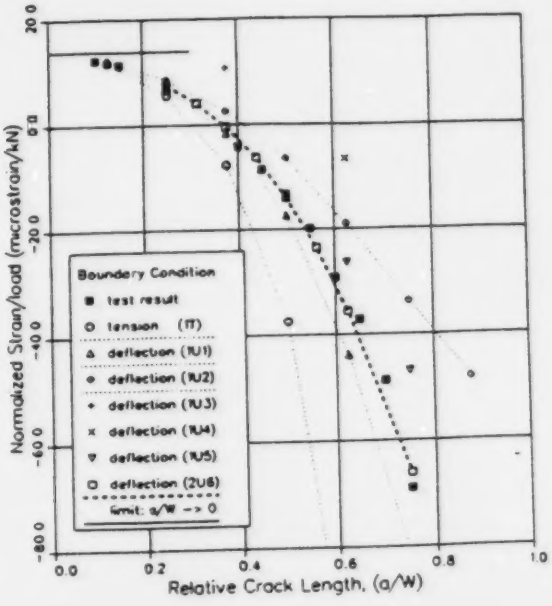

FIGURE 4

COMPARISON OF FINITE ELEMENT AND MEASURED STRAINS

5.1 *Comparison with Test Results*

Figure 3 compares crack-mouth opening deflections (CMOD) obtained from the various FE cases (open symbols) with measured values (solid symbols). Figure 4 compares predicted and measured back-face strains.

After adjusting the boundary conditions, good agreement is obtained for both CMOD and strain (case 2U6 - open squares). Strains were not predicted as well as CMOD, perhaps because their measurement is somewhat less definite than that of CMOD's (strains vary increasingly over the gauge length as the crack length increases and gauges average their value in some way), and because computed FE strains are typically less accurate than deflections/1/.

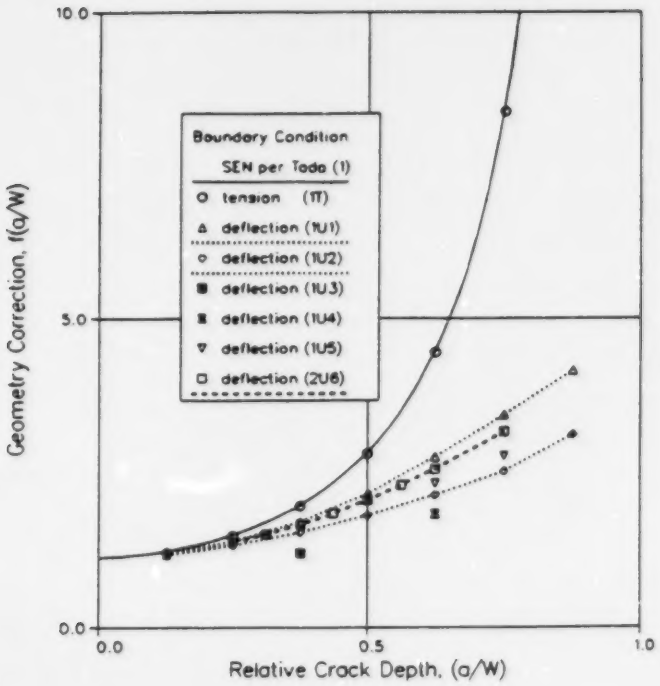

FIGURE 5

COMPARISON OF GEOMETRY "CORRECTIONS" FOR 2D SEN WITH 3D FINITE ELEMENT RESULTS WITH VARIOUS BOUNDARY CONDITIONS

5.2 *Comparison with Published Results*

In case "1T", a uniform traction was applied to the end of the FE model. Rotations were not restrained, consequently, this case corresponds to the usual SEN plate. Figures 3 and 5 also compare FE and published results/2/ for CMOD and normalized K's, showing good agreement (the geometry correction factor in Figure 5 is defined as $K/\sigma_m\sqrt{\pi a}$, where σ_m is the nominal membrane stress in the test region: $\sigma_m = P/Wt$)

5.3 *Internal Consistency of Results*

A number of numerical techniques were used to extract stress-intensity factors from "raw" FE results. These are discussed at length in Appendix C. The first of these, the virtual crack extension (VCE) technique/3/ is viewed as being the most accurate with other methods giving only slightly different results.

Case 2U6 is a refined model, otherwise identical to 1U6. Results obtained by the VCE method differed only in the fourth decimal, indicating that the models are sufficiently refined to give converged results.

Appendix C indicates that VCE results computed for successive element contours should be the same. Over three contours, a discrepancy of less than 1% in the computed J-integral, thus 0.5% in K were observed.

6.0 *RESULTS*

Table D-1 in Appendix D gives a detailed summary of FE results for a Poisson's ratio of 0.3.

Normalized stress-intensity factors are shown in Figure 5 for all cases and illustrates the following trends:

i) a general reduction in K with increased constraint

ii) the reduction increases with increasing crack length

For use in specimen testing, it is more convenient to describe the K-calibration directly in terms of the applied load. Figure 6 gives both FE results (for case 2U6) and a curve fit to the results of form:

$$K = \frac{P}{t\sqrt{W}} f(\alpha)$$

where: $f(\alpha) = 6.61\alpha - 12.6995\alpha^2 + 25.6323\alpha^3 - 12.1559\alpha^4$ (1)

$$\alpha = \frac{a}{W}$$

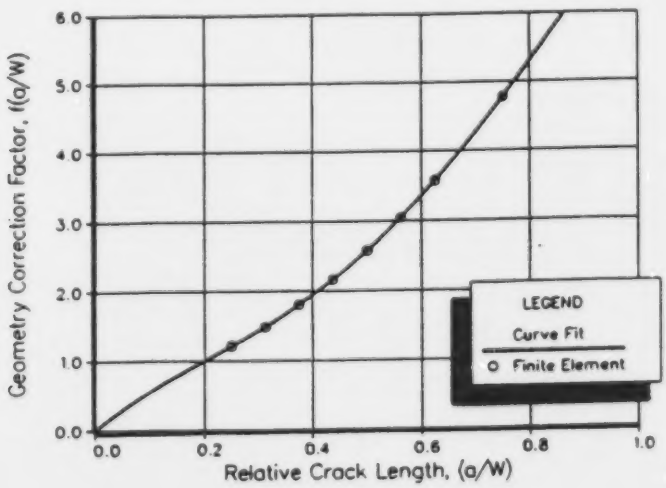

FIGURE 6

COMPARISON OF FINITE ELEMENT AND FITTED NORMALIZED K

7.0 *DISCUSSION*

The K-calibration obtained in this analysis depends on effective rotational constraint applied to the FE model which is chosen to simulate measurable quantities (the CMOD and back-face strain). These quantities in turn depend on the test fixture and testing machine bending compliances. Consequently, the K-calibration given is specific to the test configuration reported in/4/.

8.0 *CONCLUSIONS*

A 3D finite element study of a fatigue crack growth spec imen was undertaken to obtain the stress-intensity factor K as a function of load P and crack length (a/W). A significant reduction in K due to rotational constraint was observed. The amount of reduction was found to increase with crack length.

The actual amount of constraint in the specimen is not known. An effective boundary condition was determined by trial-and-error to match both the predicted and measured crack mouth opening deflection and back-face strains over the required range of a/W. Computed values of K were then curve-fitted as shown in Figure 6.

Although the technique used to obtain the K-calibration is relatively general, the calibration given by Equation 1 (Figure 6) is specific to the test configuration reported in/4/.

Approved by:

B. Mukherjee

for J. Brown
Manager
Metallurgical Research Department

Prepared by:

M.L. Vanderglas

M.L. Vanderglas
Engineer
Fracture Technology Section

Recommended by:

B. Mukherjee

B. Mukherjee
Supervising Engineer
Fracture Technology Section
Metallurgical Research Department

REFERENCES

1. Zienkiewicz, O.C., The Finite Element Method, McGraw-Hill, New York, 1971.

2. Tada, H., Paris, P.C., Irwin, G.R., The Stress Analysis of Cracks Handbook, Paris Productions Inc., St. Louis, 1985.

3. Parks, D.M., "A stiffness derivative finite element technique for determination of crack tip stress intensity factors", Int. J. Fracture, Vol. 10, 1974, pp. 487-502.

4. Lepik, O.E., Seahra, H., "Near-threshold fatigue crack propagation behaviour of Darlington Unit 2 generator rotor material", OHRD report 91-47-K, 1991.

5. Rooke, D.P., Cartwright, D.J., Compendium of Stress Intensity Factors, Her Majesty's Stationery Office, London, 1976.

6. ABAQUS User's Manual, Hibbet, Karlsson & Sorenson, Inc., Providence, Rhode Island.

7. Rice, J.R., "A path independent integral and the approximate analysis of strain concentration by notches and cracks", J. Applied Mech., Vol. 35, 1968, pp. 379-386.

8. Fenner, D.N., Abdul Mihsein, M.J., "Crack front elastic stress state for three-dimensional crack problems", Int. J. Fracture, Vol. 25, 1984, pp. 121-131.

9. Vanderglas, M.L., "A three dimensional numerical study of the effects of free surfaces on the J-integral", OHRD report 85-296-K, November, 1985.

10. Chan, S.K., Tuba, I.S., Wilson W.K., "On the finite element method in linear fracture mechanics", Eng. Fracture Mech., Vol. 2, 1970, pp. 1-17.

11. Paris, P.C., "Stress analysis of cracks", ASTM STP 381, 1970, pp. 30-81.

12. Williams, M.L., "On the stress distribution at the base of a stationary crack", J. Appl. Mech., 1957, pp. 109-114 (see also 1961, pg. 82).

13. Mowbray, D.F., "A note on the finite element method in linear fracture mechanics", Eng. Fracture Mech., Vol. 2, 1970, pp. 173-176.

APPENDIX A
2D FINITE ELEMENT STUDY OF ROTATIONAL CONSTRAINT

This appendix attempts to quantify the effects of rotational constraint on single-edge-notched (SEN) plates loaded in tension.

Published solutions exist for the SEN plate in tension and bending/2,5/ but only limited results are available for prescribed deflection and rotation boundary conditions.

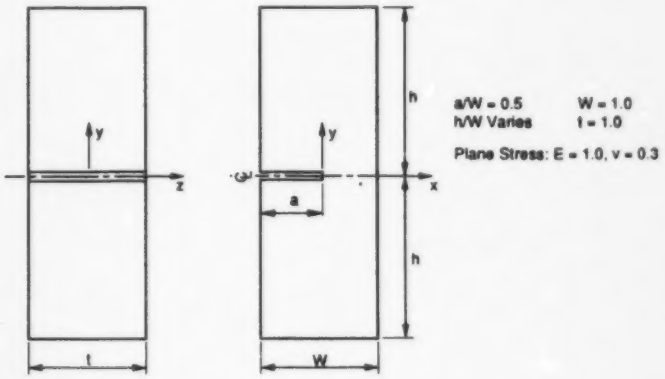

FIGURE A-1
2D SEN PLATE TEST CASE - NOMENCLATURE

Results were based on a number of two-dimensional finite element (FE) test cases in which the crack length, a, was fixed but the plate length, h, was varied. Figure A-1 shows the geometry. For simplicity, plane stress conditions with an elastic modulus, E, of 1.0 and Poisson's ratio, ν, of 0.3 were assumed. The plate width, W, was taken to be 1.0.

Three types of boundary conditions were applied to the plate ends:

i) axial force supplied by a uniform membrane stress,

ii) in-plane moment supplied by a uniform bending stress,

iii) uniform axial deflection, v, with no rotation, $v' = 0$

Conditions and results are given in Table A-1.

TABLE A-1

Single-Edge Cracked Plate (a/W = 0.5) Showing Effect of Boundary Condition Type and Plate Length on the Stress-Intensity Factor and Vertical Deflections.

1 BC	h/W	2 σ_o [Pa]	J [N/m]	K [Pa/m]	3 f	v [m] x=-0.5	x=0.0	x=+0.5
T	0.50	1.0000	14.1465	3.7612	3.001	6.329	1.807	-0.322
T	0.75	1.0000	12.6252	3.5532	2.835	5.311	2.175	-0.394
T	1.00	1.0000	12.4915	3.5343	2.820	5.353	2.500	-0.258
T	2.00	1.0000	12.4841	3.5333	2.819	6.323	3.523	0.719
T	3.00	1.0000	12.4841	3.5333	2.819	7.324	4.522	1.720
T	4.00	1.0000	12.4841	3.5333	2.819	8.324	5.522	2.720
M	0.50	1.0000	4.0987	2.0245	1.615	4.216	0.788	-1.016
M	0.75	1.0000	3.5585	1.8864	1.505	3.596	0.869	-1.476
M	1.00	1.0000	3.5107	1.8737	1.495	3.704	0.919	-1.802
M	2.00	1.0000	3.5080	1.8730	1.494	4.685	0.935	-2.818
M	3.00	1.0000	3.5080	1.8730	1.494	5.685	0.934	-3.817
M	4.00	1.0000	3.5080	1.8730	1.494	6.685	0.934	-4.817
U	0.50	1.1646	1.9736	1.4048	0.962	1.000	1.000	1.000
U	0.75	0.8158	1.3690	1.1700	1.144	1.000	1.000	1.000
U	1.00	0.6366	1.0708	1.0348	1.297	1.000	1.000	1.000
U	2.00	0.3541	0.5710	0.7556	1.703	1.000	1.000	1.000
U	3.00	0.2518	0.3740	0.6116	1.938	1.000	1.000	1.000
U	4.00	0.1974	0.2675	0.5172	2.091	1.000	1.000	1.000
U	5.00	0.1630	0.2018	0.4493	2.199	1.000	1.000	1.000
U	6.00	0.1392	0.1581	0.3976	2.279	1.000	1.000	1.000
U	7.00	0.1216	0.1273	0.3567	2.341	1.000	1.000	1.000
U	8.00	0.1081	0.1048	0.3237	2.389	1.000	1.000	1.000
U	9.00	0.0973	0.0878	0.2963	2.430	1.000	1.000	1.000
U	10.00	0.0885	0.0746	0.2732	2.463	1.000	1.000	1.000

1) type of boundary condition:
   "T" - prescribed traction
   "M" - prescribed moment
   "U" - prescribed deflection
2) σ_o = membrane or bending stress or P/tW for prescribed deflection cases (where P is the reaction force)
3) geometry "correction" factor: $f = K/\sigma_o\sqrt{\pi a}$
4) f = 2.8266 for tension and f = 1.4752 for bending per /2/

All cases are plane stress with E = 1.0 Pa, ν = 0.3.

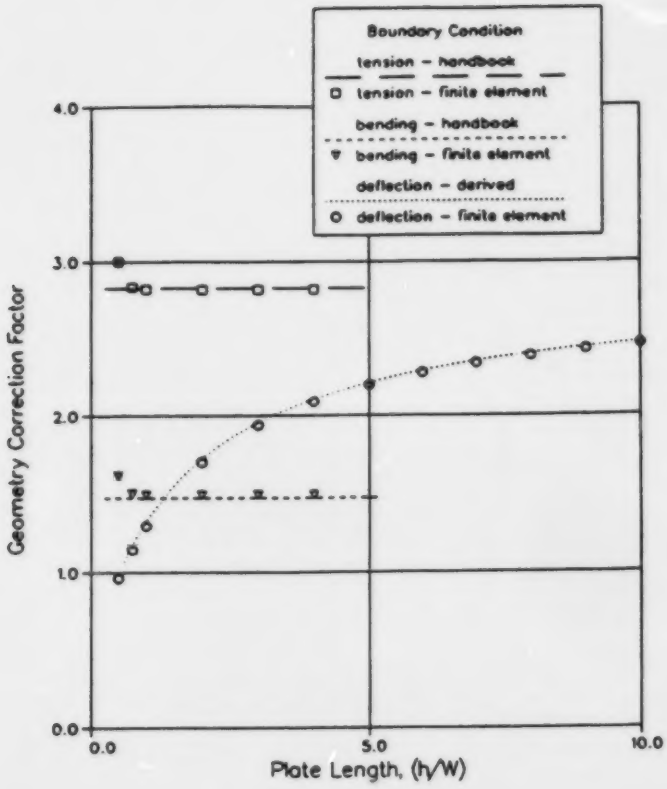

FIGURE A-2

COMPARISON OF GEOMETRY CORRECTION FACTORS FOR 2D SEN PLATES WITH TENSION, BENDING AND DEFLECTION BOUNDARY CONDITIONS - EFFECT OF PLATE LENGTH

The stress-intensity factors for the membrane and bending cases are, in normalized form:

$$\frac{K_m}{\sigma_m\sqrt{\pi a}} = f_m; \frac{K_b}{\sigma_b\sqrt{\pi a}} = f_b \qquad \text{(A-1)}$$

where f_m and f_b are dimensionless geometry "correction" factors which may depend on the relative crack length (a/W) and plate length (h/W), and σ_m and σ_b are the nominal membrane and bending stress, respectively.

Computed values of f_m and f_b are compared to a handbook solution/2/ in Figure A-2 for a range of h/W. For h/W > 1, computed results no longer change with plate length and are the same as the handbook solutions.

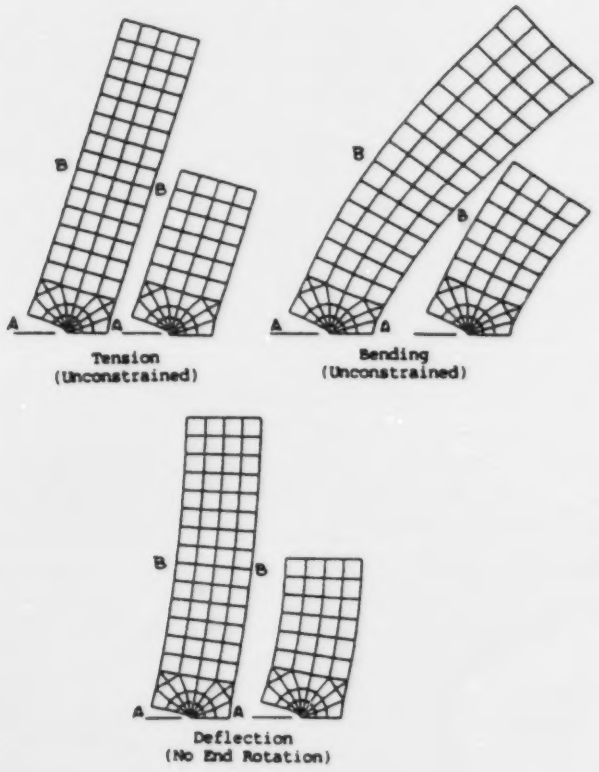

FIGURE A-3

2D SEN PLATE TEST CASE - "DEFORMED" MESHES OF SHORT AND LONG PLATES WITH VARIOUS BOUNDARY CONDITIONS (A-A IS SYMMETRY PLANE)

Figure A-3 compares the deflected shapes of a short and long plate for each of the three boundary condition types. The deflections in the region A-A-B-B of a long plate loaded in tension are essentially identical to those in a shorter plate. The same pertains to the bending case but not to the prescribed deflection case since the rotation is zero at the end of the plates, not along B-B in the longer plate.

In the tension case, the portion of the plate above (about) y/b = 1 exhibits a rigid body translation and rotation plus a simple tensile extension. In the bending case, a translation and rotation plus pure bending is observed. The average deflection and rotation (actually slope) at the remote end of the plates can be represented in the form:

tension:	deflection	$= v_m = A\sigma_m + (h/W)\sigma_m$	(A-2)
	rotation	$= v'_m = B\sigma_m$	(A-3)
bending:	deflection	$= v_b = C\sigma_b$	(A-4)
	rotation	$= v'_b = D\sigma_b + (2h/EW)\sigma_b$	(A-5)

where: A = 1.522, B = 5.600, C = 0.934 and D = 3.500

where the terms ($h\sigma_m/E$) and ($2h\sigma_b/EW$) are the extension and rotation of a rectangular bar in simple tension and bending, respectively. The remaining terms are extensions and rotations attributable to the presence of the crack and are viewed as being independent of the plate length.

Figure A-4 compares Equations A-2 to A-5 (dotted lines) with FE results (symbols) to demonstrate that the equations provide a viable representation.

The total stress-intensity factor for combined tension and bending is:

$$K = (\sigma_m f_m + \sigma_b f_b)\sqrt{\pi a}$$

or (A-6)

$$\frac{K}{\sigma_m\sqrt{\pi a}} = f_m + (\sigma_b/\sigma_m)f_b = f_{net}$$

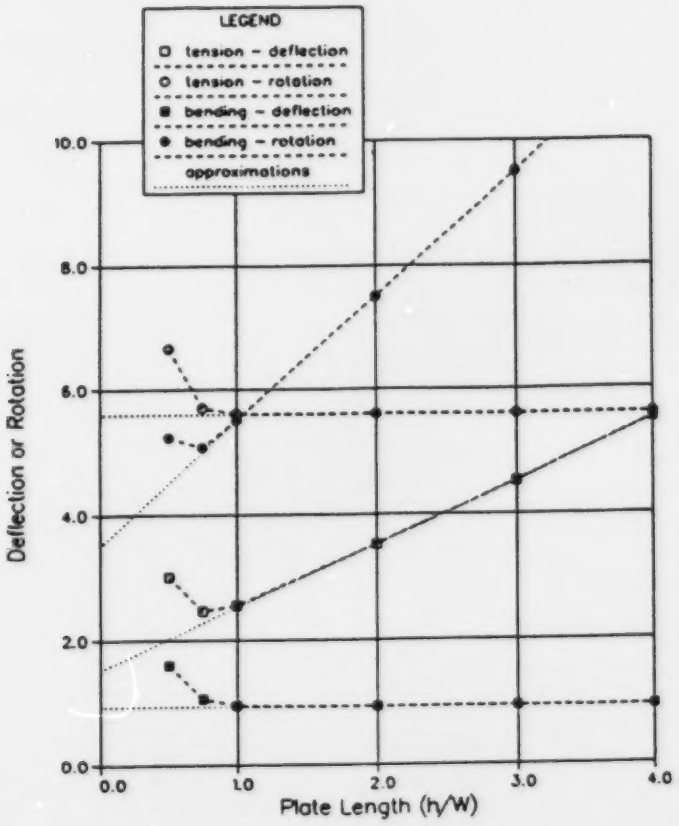

FIGURE A-4

DEFLECTIONS AND ROTATIONS IN 2D SEN PLATES IN TENSION AND BENDING - EFFECT OF PLATE LENGTH

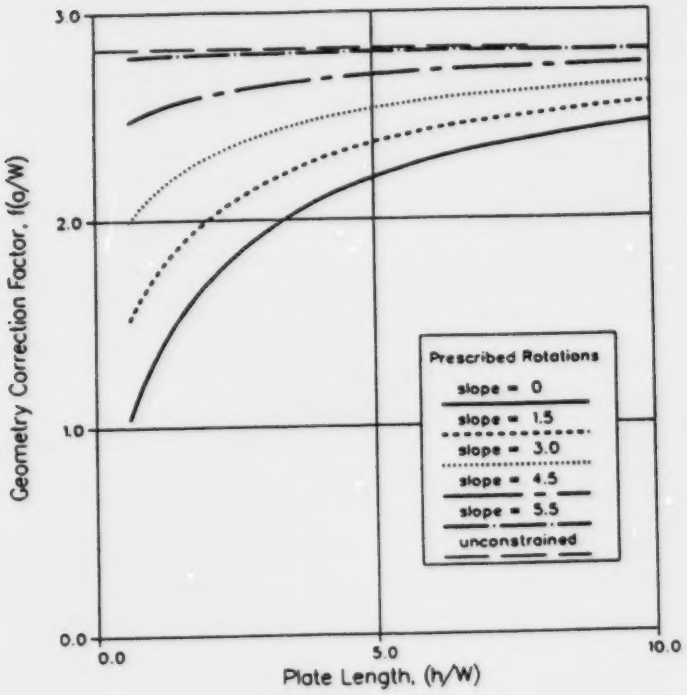

FIGURE A-5

GEOMETRY CORRECTION FACTORS FOR 2D SEN IN TENSION
WITH CONSTRAINED END ROTATIONS
(ROTATION IN UNCONSTRAINED PLATE IS 5.6)

Figure A-2 also compares FE results and those derived from Equations A-2 to A-5 for the case: (v = 1, v' = 0) to verify those equations. (The derived result was obtained by summing the deflections and rotations in Equations A-2 to A-5, then solving for the induced membrane and bending stress and inserting the latter into Equation A-6). Figure A-5 shows results for a case in which a membrane stress is prescribed and the rotation is varied.

To obtain a solution for K for tension in which the rotation is constrained, Equations A-3 and A-5 can be added and solved for σ_b, now regarded as a "reaction" or "induced" bending stress:

$$\sigma_b = \frac{v' - B\sigma_m}{D + (2h/EW)} \qquad \text{(A-7)}$$

where: σ_b = prescribed membrane stress
v' = prescribed rotation

Figure A-6 shows the ratio of the induced bending to applied membrane stress for plates of various lengths obtained using Equation A-7 for various rotations. Note that the induced bending stress is negative (i.e. tends to close the crack) but decreases in magnitude with increasing plate length. Consequently, the overall geometry correction factor f_{net} in Equation A-6 is less than the membrane correction.

For a plate with no crack, the constants A, B, C and D in Equations A-2 to A-5 (and also K) are zero. Thus the magnitude of the induced bending stress and thus the difference between K for specimens loaded in tension with and without rotational constraint varies with crack length.

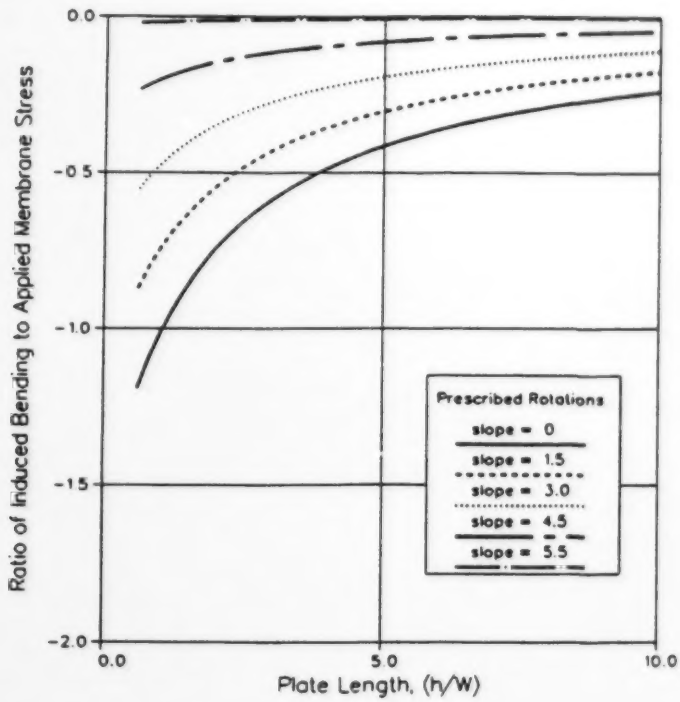

FIGURE A-6

INDUCED BENDING STRESS IN 2D SEN PLATES IN TENSION
WITH CONSTRAINED END ROTATIONS
(ROTATION IN UNCONSTRAINED PLATE IS 5.6)

APPENDIX B
FINITE ELEMENT DETAILS

Results were obtained using a proprietary finite element code (ABAQUS version 4-8.5/6/).

The material was assumed to be isotropically elastic with an elastic modulus of 200 GPa and Poisson's ratio of 0.3.

All 3D models have two planes of symmetry. Although the actual specimen/load-fixture arrangement is not completely symmetrical with respect to the crack plane, this asymmetry was ignored.

Results were obtained for a range of crack lengths using two FE model types. These differ in the degree of mesh refinement near the crack plane. Typical meshes are shown in Figure 2.

All 3D models used second order pentahedral and hexahedral elements (ABAQUS "C3D15" and "C3D20" types). A typical crack tip detail, (also shown in Figure 2), includes a layer of surface elements to detect the strong through-thickness variation of strains near the free surface.

The hexahedral elements bordering the crack front were "collapsed" into a wedge shape; the coincident nodes resulting were constrained to move as one by enforcing "multi-point" constraints ("MPC's"). In addition, the near-tip elements were converted to "quarter-point" types/1/.

Mesh generation, and pre- and post-processing operations were performed using a variety of "in-house" computer programs.

APPENDIX C
CALCULATION OF K BY ALTERNATIVE METHODS

To verify the K-calculation, several independent numerical techniques were used to extract stress-intensity factors from the FE solutions. These vary in accuracy. The first method, which is viewed to be the most accurate, was used in all cases, the others as "spot checks" for selected cases.

C-1 *Virtual Crack Extension (VCE)*

In all cases, K was calculated by first using the "virtual crack extension" (VCE) method/3/ (an ABAQUS output option) to obtain the J-integral, J, then using the elastic relation/7/ to convert J to K:

$$K = \sqrt{E'J} \qquad \text{(C-1)}$$

Several values of J can be computed in a single analysis, each derived from a single contour of elements surrounding the crack tip. In theory, these should be identical. The extent of their actual agreement (e.g. their "path-independence") gives some indication of the adequacy of the FE mesh. Computed values of J varied by less than 1%, thus K's are consistent to within 0.5% because of the square-root relation between K and J.

Two difficulties attend this calculation when applied to 3D analysis:

i) since, in general, 3D fields differ from both plane stress or plane strain, the appropriate value of the effective modulus (E' in Equation C-1) to be used in converting J to K is somewhat arbitrary and may be thickness-dependent

ii) when Poisson's ratio is non-zero, the computed values of J will vary along the crack front even if the front is straight and the crack is subjected to nominal stresses which do not vary in the thickness direction/8/

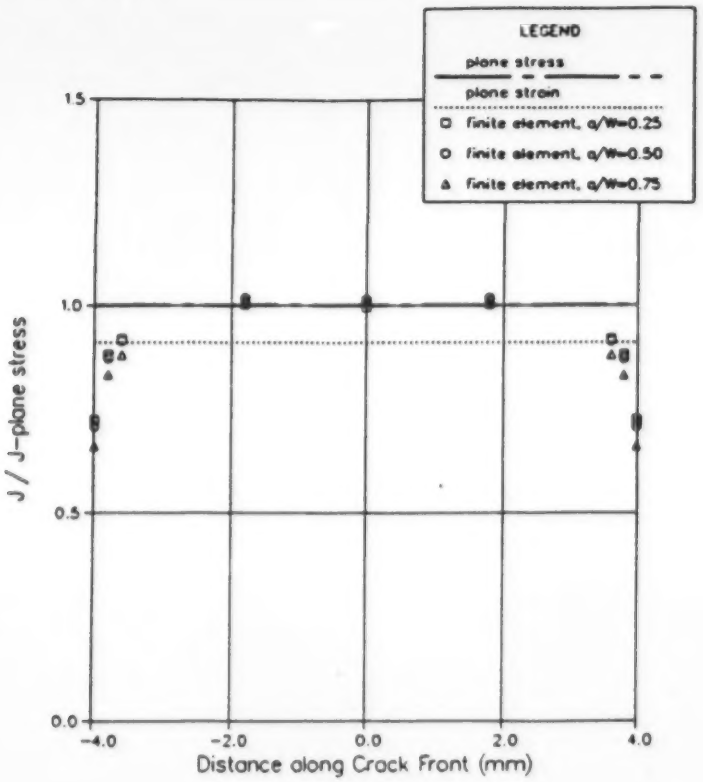

FIGURE C-1

J-VARIATIONS ALONG CRACK FRONT - COMPARISON WITH PLANE-STRESS AND PLANE-STRAIN RESULTS FOR EDGE-CRACKED PLATE IN TENSION

Figure C-1 compares local J-integral values for three crack lengths obtained by the VCE method to plane-stress and plane strain results/2/ for a specimen loaded in tension (case "1T" in Table 1). Over most of the crack front, local values are nearest the 2D plane-stress result.

Variations in J along the crack front lead to several problems:

i) the measured growth rates results are to be interpreted as a function of a single parameter, K, thus it is necessary to convert the distribution of J along the crack front to a single value of J, thus K

ii) a previous numerical study/9/ revealed that coarse through-thickness discretizations of the FE model could produce J-distributions radically different from more refined models

iii) the path independence of contours on a single layer may be lost

These difficulties are remedied upon noting that in 3D applications, it is the total change in energy with the entire crack area which controls the specimen behaviour. This quantity can be obtained by integrating the numerically-determined "local" values of J along the crack front, then dividing by the length of the front. For second order elements with straight crack fronts, the result is given by a sum over all elements bordering the crack front/9/:

$$J_{avg} = (1/t)\sum\int_{-1}^{+1} N^P(\zeta)\, J^P\, t_e d\zeta \qquad \text{(C-2)}$$

where: J^P = nodal values of J resulting from the VCE procedure
N^P = shape functions along the crack front given by

$N^1 = -(\zeta/2)(1 - \zeta)$
$N^2 = 1 - \zeta^2$
$N^3 = +(\zeta/2)(1 + \zeta)$

ζ = local coordinate along crack front
t = specimen thickness
t_e = length of crack front spanned by one element

The integrated average value of J (using Equation C-2) for case "1T" was within -1.6% to -2.8% of the plane stress value but +6.8% to 8.2% of the plane strain value, depending on crack length.

Displacement Substitution/10/

This method was used only for a few cases as an independent check on the previous method. The asymptotic form of the crack face opening deflection, v, approaching the crack tip is always/11,12/ (for symmetric, opening-mode cases):

$$v = \frac{K}{E'}\sqrt{\frac{8r}{\pi}} \qquad \text{(C-3)}$$

where r is the distance to the crack tip.

The radius and computed opening deflection for some crack face node is inserted into Equation C-3 and a trial value of K, say K*, is evaluated from:

$$K^* = E'v\sqrt{\frac{\pi}{8r}} \qquad \text{(C-4)}$$

A plot of K versus r is prepared by repeating the process for a series of nodes. Extrapolating the plot to r = 0 gives an estimate of K.

Figure C-2 compares results obtained by both the VCE and displacement substitution methods for three crack lengths.

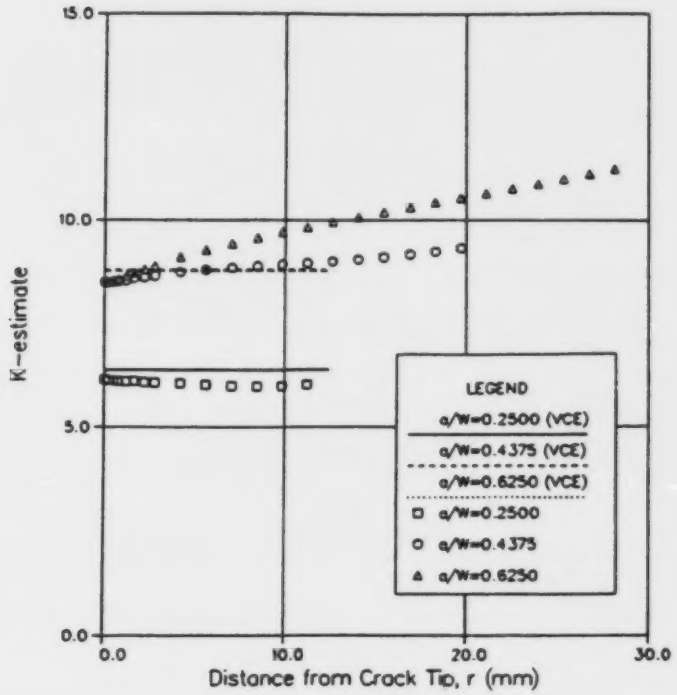

FIGURE C-2

COMPARISON OF VCE AND DISPLACEMENT SUBSTITUTION METHODS - DEFLECTION BC (1.0 mm) APPLIED AT x=105.6 mm - CASE 206

The method works well for 2D applications, but the same difficulty in choosing an appropriate value of the effective modulus, E', noted in the Appendix C-1 again arises. In addition, since the lateral strains vary approaching the crack front, the deviation from plane stress or strain and thus the "correct" value of E' may vary with r. Consequently, this technique is viewed to be inferior to the VCE method and is used only as a crude estimator of K.

C-3 *Compliance*

This method (similar to Mowbray/13/) was used only for cases in which prescribed deflection boundary conditions were specified. For a fixed deflection, v, the load P decreases with crack length. Defining the compliance as

$$C = v/P \tag{C-5}$$

the work done is (with v the deflection of half the specimen measured relative to the crack plane)

$$\text{Work} = Pv = v^2/C \tag{C-6}$$

The stress-intensity factor K is related to the change in work with crack area, A, as follows:

$$\frac{K^2}{E'} = -\frac{\partial \text{Work}}{\partial A} = +\left(\frac{v}{C}\right)^2 \frac{\partial C}{\partial A} \tag{C-7}$$

The specimen thickness, t, is assumed to be constant thus the crack area is

$$A = at \tag{C-8}$$

Denoting the relative crack length (a/W) by α, Equation C-7 can be written in the form:

$$\frac{K^2}{E'} = \frac{1}{Wt}\left(\frac{v}{C}\right)^2 \frac{\partial C}{\partial \alpha} \tag{C-9}$$

The load at the location at which the deflections are prescribed was obtained by summing the computed reactions on that section. Computed compliances were then curve-fitted as a function of relative crack length, α in the form:

$$C = 1.13926 - 1.38466\alpha + 7.56397\alpha^2 - 13.2526\alpha^3 + 15.7881\alpha^4 \text{ [mm/kN]} \tag{C-10}$$

where: $0.25 < \alpha < 0.75$

whose derivative is:

$$\frac{\partial C}{\partial \alpha} = -1.38466 + 15.12794\alpha - 39.7578\alpha^2 + 63.1524\alpha^3 \text{ [mm/kN]} \qquad \text{(C-11)}$$

These expressions were inserted into Equation C-9 to obtain K as a function of α (for case "2U6" in Table 1). Figure C-3 compares the result (solid curve) with computed values of K obtained using the VCE technique (symbols) and demonstrates good agreement.

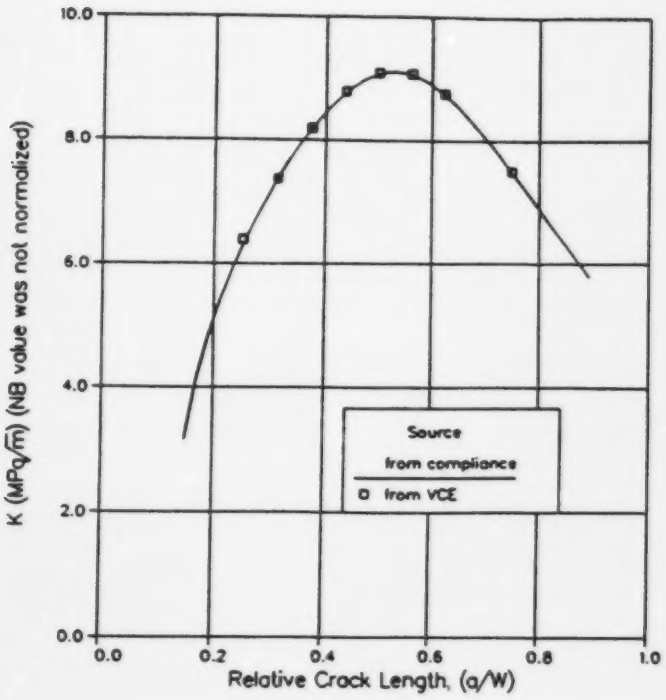

FIGURE C-3

COMPARISON OF K'S FROM VCE AND COMPUTED COMPLIANCE - DEFLECTION BC (1.0 mm) APPLIED AT z=105.6 MM - CASE 2U6

C-4 *Selection of the Effective Modulus, E'*

In all three methods described in this appendix, it is necessary to specify a value of E'. The limiting values are:

$$\text{where: } E' = \begin{cases} E \text{ for plane stress} \\ E/(1-\nu^2) \text{ for plane strain} \end{cases} \qquad \text{Equation C-12}$$

These differ by about 9% (for $\nu = 0.3$).

A comparison of FE and 2D values of J was shown in Figure C-1. Crack-front averaged values were intermediate between plane-stress and plane-strain but tended to the former.

Figure C-4 compares values of CMOD for a range of crack depths, obtained by FE analysis for model "1T" to published/2/ 2D results. The deflections vary by several orders of magnitude, thus the percentage differences between FE and 2D results are shown. Again, the 3D FE results tend to the 2D plane stress results.

For these reasons, the elastic modulus was used when converting quantities such as the J-integral to K (i.e. E' = E was selected).

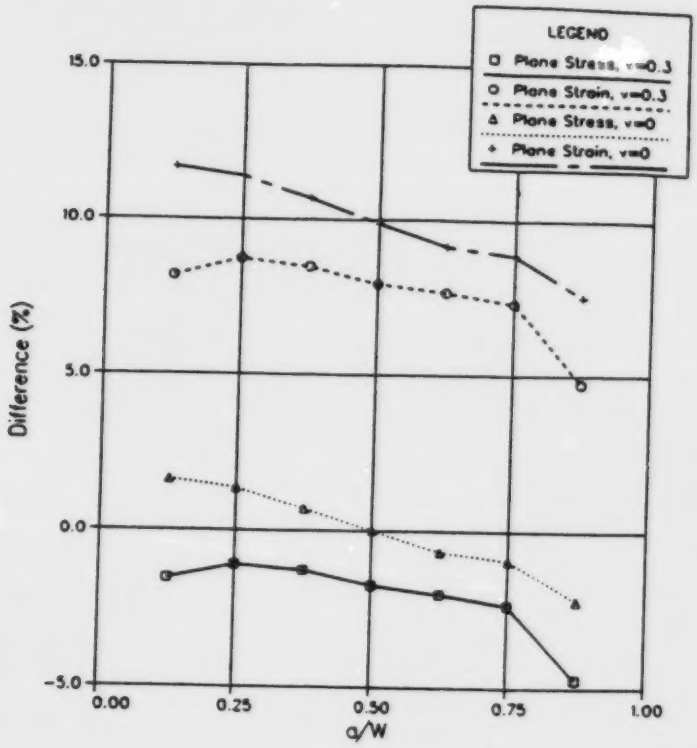

FIGURE C-4

CRACK MOUTH OPENING DEFLECTIONS - COMPARISON OF FINITE ELEMENT WITH PLANE-STRESS AND PLANE-STRAIN SOLUTIONS

APPENDIX D
3D SPECIMEN ANALYSIS - SUMMARY OF RESULTS

Table D-1 contains a summary of the finite element results for the 3D specimen. The following variables are listed:

Case.... described in Table 1
a/W..... relative crack length
J..... J-integral as computed by the VCE method, averaged over the crack front
K..... stress-intensity factor computed as EJ where E is Young's modulus (200 GPa)
f(a/W).. geometry correction factor (see Figure 6)
P..... total applied or reaction force
CMOD.... crack mouth opening deflection
ϵ..... back-face strain
v..... prescribed deflection boundary condition

TABLE D-1

Summary of 3D Finite Element Results (Poisson's Ratio = 0.30)

Case	a/W	J (N/m)	K (MPa/m)	K/Ko	P (kN)	CMOD (mm)	CMOD/P (mm/kN)	ϵ/P ($\mu\epsilon$/kN)	V end deflection (m)
1T	0.1250	0.2519	0.224	0.7516	0.50680	0.2472E-03	0.4878E-03	11.77	-
1U1	0.1250	68.7927	3.709	0.7396	8.51060	0.4080E-02	0.4794E-03	12.06	0.1000E-04
1U2	0.1250	66.7881	3.655	0.7286	8.51280	0.4015E-02	0.4716E-03	12.33	0.1000E-04
1T	0.2500	0.7626	0.391	1.3077	0.50680	0.6315E-03	0.1246E-02	5.62	-
1U1	0.2500	167.9160	5.795	1.2303	7.99360	0.9282E-02	0.1161E-02	7.27	0.1000E-04
1U2	0.2500	152.3890	5.521	1.1670	8.02800	0.8760E-02	0.1091E-02	8.64	0.1000E-04
1U6	0.2500	203.8720	6.385	1.2140	8.92640	0.1020E-01	0.1143E-02	7.62	0.1000E-04
2U6	0.2500	203.8210	6.385	1.2139	8.92560	0.1021E-01	0.1144E-02	7.66	0.1000E-04
2U6	0.3125	271.2960	7.366	1.4895	8.39260	0.1356E-01	0.1616E-02	4.15	0.1000E-04
1T	0.3750	2.0144	0.635	2.1254	0.50680	0.1381E-02	0.2725E-02	-7.76	-
1U1	0.3750	289.9860	7.616	1.8547	6.96820	0.1607E-01	0.2306E-02	-1.70	0.1000E-04
1U2	0.3750	244.8990	6.999	1.6646	7.13500	0.1435E-01	0.2011E-02	2.56	0.1000E-04
1U3	0.3750	0.7502	0.387	1.2971	0.50680	0.7293E-03	0.1439E-02	10.71	0.6520E+01
1U6	0.3750	335.7280	8.194	1.8032	7.71200	0.1716E-01	0.2226E-02	-0.54	0.1000E-04
2U6	0.3750	335.4990	8.191	1.8029	7.71060	0.1717E-01	0.2227E-02	-0.44	0.1000E-04
2U6	0.4375	386.5470	8.793	2.1634	6.89720	0.2087E-01	0.3026E-02	-6.37	0.1000E-04
1T	0.5000	5.5060	1.049	3.5139	0.50680	0.3063E-02	0.6044E-02	-37.48	-
1U1	0.5000	376.3460	8.676	2.7037	5.44560	0.2364E-01	0.4341E-02	-17.38	0.1000E-04
1U2	0.5000	307.3830	7.841	2.2636	5.87840	0.2009E-01	0.3417E-02	-6.47	0.1000E-04
1U6	0.5000	414.1550	9.101	2.5756	5.99680	0.2442E-01	0.4072E-02	-14.20	0.1000E-04
2U6	0.5000	413.9190	9.099	2.5757	5.99480	0.2443E-01	0.4075E-02	-13.96	0.1000E-04
2U6	0.5625	412.7320	9.086	3.0462	5.06160	0.2759E-01	0.5451E-02	-23.57	0.1000E-04
1T	0.6250	17.2490	1.857	6.2195	0.50680	0.7489E-02	0.1478E-01	-112.28	-
1U1	0.6250	361.1270	8.499	3.8464	3.74960	0.3006E-01	0.8016E-02	-43.87	0.1000E-04
1U2	0.6250	309.2370	7.864	2.9844	4.47200	0.2487E-01	0.5561E-02	-19.04	0.1000E-04
1U4	0.6250	453.0350	9.519	2.5540	6.32500	0.2742E-01	0.4335E-02	-6.63	0.1000E-04
1U5	0.6250	409.6260	9.051	3.2397	4.74140	0.2981E-01	0.6288E-02	-26.39	0.1000E-04
1U6	0.6250	384.4740	8.769	3.5728	4.16520	0.3014E-01	0.7237E-02	-35.99	0.1000E-04
2U6	0.6250	384.2090	8.766	3.5733	4.16320	0.3015E-01	0.7242E-02	-35.57	0.1000E-04

TABLE D-1 (Continued)

Summary of 3D Finite Element Results (Poisson's Ratio = 0.30)

Case	a/W	J (N/m)	K (MPa/m)	K/Ko	P (kN)	CMOD (mm)	CMOD/P (mm/kN)	ϵ /P ($\mu\epsilon$/kN)	end deflection (m)
1T	0.7500	73.4409	3.833	12.8335	0.50680	0.2262E-01	0.4463E-01	-348.84	-
1U1	0.7500	262.8000	7.250	5.2727	2.33340	0.3358E-01	0.1439E-01	-83.32	0.1000E-04
1U2	0.7500	261.5410	7.232	3.8599	3.17980	0.2779E-01	0.8741E-02	-33.70	0.1000E-04
1U5	0.7500	305.3580	7.815	4.2385	3.12900	0.3209E-01	0.1026E-01	-47.01	0.1000E-04
1U6	0.7500	280.8100	7.494	4.7819	2.65960	0.3305E-01	0.1243E-01	-66.07	0.1000E-04
1T	0.8750	690.3150	11.750	39.3458	0.50680	0.1169E+00	0.2307E+00	-1762.15	-
1U1	0.8750	159.6000	5.650	6.8652	1.39660	0.3395E-01	0.2431E-01	-134.30	0.1000E-04
1U2	0.8750	209.2380	6.469	5.1473	2.13280	0.2855E-01	0.1339E-01	-48.18	0.1000E-04